Ultrabroadband few-cycle infrared pulse generation from a noncollinear optical parametric amplifier based on bulk niobate crystals

Oleksandr Isaienko and Eric Borguet*

Chemistry Department, Temple University, 1901 North 13th Street, Philadelphia, Pennsylvania 19122, USA
**Corresponding author: eborguet@temple.edu*

Received March 14, 2013; revised May 23, 2013; accepted May 27, 2013;
posted June 4, 2013 (Doc. ID 187049); published July 11, 2013

We describe a near-IR two-stage noncollinear optical parametric amplifier (NOPA) pumped at 800 nm that employs bulk congruent lithium niobate [$LiNbO_3$ (c-LNB)] and bulk potassium niobate [$KNbO_3$ (KNB)] crystals. Noncollinear phase matching in these materials allows for generation of pulses as broad as 2900 cm^{-1} (~78 THz) centered in the near-IR at ~1300 nm. In the particular geometry described here, the LNB crystal amplifies the white-light seed continuum, and the KNB crystal further amplifies the broadband near-IR pulses. Use of pulse-front matching at both nonlinear optical crystals allows for improvement of the spatiotemporal profile of the amplified ultrabroadband signal pulses and their compression to ≤22 fs. Because of the relatively high nonlinear coefficients of these crystals, we achieve overall amplification efficiencies >7% in two consecutive NOPA stages.

OCIS codes: (160.3730) Lithium niobate; (190.4410) Nonlinear optics, parametric processes; (190.7110) Ultrafast nonlinear optics; (190.4223) Nonlinear wave mixing; (320.7110) Ultrafast nonlinear optics.
http://dx.doi.org/10.1364/JOSAB.30.002075

1. INTRODUCTION

The development of methods devoted to the generation of broadband ultrashort pulses in the near- and mid-IR frequency ranges has recently seen considerable growth. One of the strongest motivations has been the prospect of increasing the cutoff frequency of x-ray pulses generated via high-harmonic generation [1–3]. Nonlinear wave-mixing methods, such as optical parametric amplification (OPA), difference frequency generation, and four-wave mixing, have proven very versatile for the generation of broadband laser radiation tunable over a wide frequency range from the visible to terahertz waves [4–14]. By selecting an appropriate nonlinear material, pump wavelength, and geometry for a particular nonlinear process, one can control the bandwidth of the parametric process and generate extremely broadband pulses over a wide spectral range [11]. The central wavelength, as well as the bandwidth of the generated pulses, in general, do not depend on the absorption or emission properties of a given nonlinear optical material, but are rather defined by the dispersion properties and the geometry of the beams with respect to the nonlinear crystal's axis (axes).

The major parameter that defines the parametric bandwidth of the OPA process is the phase mismatch $\Delta k = |k_p - k_s - k_i|$ among the interacting pump, signal, and idler waves (with the traditional notation $\omega_p > \omega_s > \omega_i$). The efficiency of parametric amplification strongly depends on the phase mismatch: it reaches a maximum when $\Delta k = 0$, and decreases rapidly as Δk deviates from zero [4]. Thus, one can propose a criterion for the bandwidth of amplification such that when the modulus of Δk falls within a certain range of values, the corresponding frequencies will be phase matched, and thus amplified. Such a criterion can be set as follows [4,15,16]: $|\Delta k \cdot l_c| \leq \pi$, where l_c is a characteristic interaction length among the three waves, typically the length of the nonlinear crystal. In the case of OPA, the bandwidth of the amplified pulses is defined, to the first dispersion order of the phase mismatch, in the following way:

$$\Delta\omega_s = \frac{\pi}{l_c} \frac{1}{\left|\frac{1}{v_i} - \frac{1}{v_s}\cos(\alpha+\beta)\right|}, \tag{1}$$

where v_s and v_i are the group velocities of signal and idler, and α and β are the noncollinear angles between signal and pump and between idler and pump, respectively. By matching the group velocities of signal and idler, one can achieve extreme broadening of signal (and idler) from an OPA [4,15,17]. The broadening of amplified pulses is naturally achieved in type-I OPA at the degeneracy point. More importantly, the group-velocity matching for signal and idler can be achieved at wavelengths away from degeneracy by employing noncollinear phase matching (noncollinear OPA, commonly known as NOPA), which is the object of the current discussion. Finally, a special case of broadband phase matching for type-I OPA occurs when the degeneracy wavelength matches the zero-dispersion wavelength of the nonlinear optical material: the bandwidth in this case becomes defined by the fourth-order dispersion, which is normally much smaller than the second-order term (the first- and third-order terms are zero at degeneracy in type-I OPA) [18],

$$\Delta\omega_s = \sqrt[4]{(\pi/l_c) \cdot 1/(1/24 \cdot \partial^4 \Delta k/\partial\omega_s^4)}, \tag{2}$$

and, as a result, the bandwidth is substantially increased. Nonlinear materials, such as beta-barium borate (BBO) and bismuth borate (BiBO) are of particular interest, as they create favorable conditions to meet such requirement ($2\lambda_p = \lambda|_{\mathrm{GVD}=0}$) when pumped at the fundamental output of Ti:sapphire amplifiers [18–21].

Other methods reported recently toward broadband IR pulse generation include difference-frequency-generated seed followed by broadband OPA [22], direct amplification of seed at longer wavelengths in noncollinear geometry [23], and precompensation of the idler angular dispersion in NOPAs [24], as well as optical pulse synthesis of outputs from synchronized broadband OPAs [25]. While the methods of four-wave mixing demonstrate fewer restrictions on the amplification bandwidths owing to more relaxed phase-matching conditions [26–30], the efficiency of four-wave mixing methods (which rely on the third-order nonlinearity) is typically an order of magnitude less than for methods based on the second-order nonlinear processes.

The approaches for NOPA described above have been implemented over recent years in various nonlinear optical schemes to generate broadband ultrashort near-IR pulses. Dwayne Miller's group demonstrated a noncollinear chirped-pulse OPA in potassium-titanyl arsenate, $KTiOAsO_4$, resulting in the generation of pulses at 1.56 μm with energies of ~500 μJ [31]; however, the bandwidths achieved in their setup were limited by the narrowband seed to ~250 cm^{-1}, thus limiting the shortest pulse duration to ~70 fs. Cirmi *et al.* introduced engineered nonlinear crystals, such as periodically poled stoichiometric lithium tantalate, that would perform as near-IR NOPAs pumped at the fundamental output of a Ti:sapphire laser [32] and experimentally demonstrated generation of 8.5 fs pulses centered at ~1.3 μm [33]. In parallel, the method of broadband OPA when $2\lambda_p$ matches the zero-dispersion point was applied by the Cerullo group [19] and the team of researchers at the Max Born Institute [18] to Ti:sapphire-laser-pumped type-I OPAs based on BBO and BiBO, respectively. This method of ultrabroadband type-I OPA allowed, in particular, generation of pulses as short as ~8.5 fs with a central wavelength ~1.6 μm [19].

We introduced an 800 nm pumped type-II NOPA based on bulk potassium-titanyl phosphate (KTP) crystal and demonstrated generation of ultrabroadband pulses with bandwidths as large as 2500 cm^{-1} [34] and pulse durations <25 fs after applying pulse-front matching [35]. The particularly broad bandwidth from the type-II KTP-NOPA was achieved by making the signal seed beam divergent at the nonlinear crystal so that the multitude of noncollinear angles within the seed beam could be phase matched simultaneously. Almost at the same time, Nienhuys and Bakker reported NOPA in KTP, albeit with narrower bandwidths due to longer crystals used [36]. Subsequently, we generated ultrabroadband idler pulses from the KTP-NOPA in the 2–3 μm range [37] and extended the near-IR KTP-NOPA to the regime of high pulse repetition rates (250 kHz) [38].

In this study, we implement the method of near-IR type-I NOPA in other nonlinear materials and achieve improved performance. Lithium niobate [$LiNbO_3$ (LNB)] and potassium niobate [$KNbO_3$ (KNB)] are especially attractive materials for several reasons, including their dispersive properties for broadband phase matching in the IR and relatively high nonlinear coefficients ($d_{22} = 2.46$ pm/V and $d_{31} = -4.64$ pm/V for LNB; $d_{33} = -12$ pm/V [39,40]). In addition, LNB is readily available as a nonlinear material with a well-developed growth procedure and can be produced in various crystalline modifications. LNB and KNB have been used as efficient nonlinear crystals for the generation of femtosecond pulses in the ~2–4 μm wavelength region [39,41,42]. While BBO and BiBO have become the major crystals for the efficient parametric amplification of pulses in the near-IR ($\lambda \sim 1100$–2600 nm), lithium and potassium niobates allow one to extend pulse generation to longer wavelengths in the mid-IR. Compared to the mentioned borates, the niobates have the disadvantage of lower damage thresholds, which can be overcome, in particular, in LNB by doping it with MgO. Recently, we demonstrated generation of broadband mid-IR pulses ($\lambda \approx 2$–3.5 μm) with bandwidths up to 1500 cm^{-1} from the OPA based on LNB and KNB crystals that were applied to broadband sum-frequency vibrational spectroscopy of water/mineral interfaces [43]. The potential of these crystals for ultrabroadband near-IR generation in NOPA, when seeded with continuum, has not been fully explored, even though attempts have been mentioned in the literature [28]. In the current paper, we experimentally demonstrate the generation of ultrabroadband near-IR pulses from an 800 nm pumped NOPA based on bulk KNB and congruent LNB (c-LNB) crystals. The pulses cover the 1100–1600 nm wavelength region with bandwidths >2900 cm^{-1} (corresponding to a transform-limit ~9 fs). The application of pulse-front matching [17,35] to the NOPA in LNB and KNB allows for compression of the near-IR pulses to ~20 fs.

2. PHASE MATCHING IN $KNbO_3$ AND CONGRUENT $LiNbO_3$

The dispersive properties of LNB and KNB allow group-velocity matching between the near-IR signal and the faster mid-IR idler pulses in a noncollinear geometry when pumped at or around 800 nm, thus increasing the bandwidth of OPA process [32]. In particular, the group-velocity dispersion of these materials equals zero at 1.92 μm [32] for LNB and ~1.98 μm for KNB [44]. Thus, we expect group-velocity matching between the near-IR signal and the mid-IR idler in these materials when pumped at the fundamental output of Ti:sapphire lasers [32].

For KNB, the most efficient phase matching with an 800 nm pump occurs in the ZX plane ($\varphi = 0°$, θ can vary). Here, the optical axes XYZ of this $mm2$-symmetry biaxial crystal are assigned to the crystallographic axes, abc, in the following order: $X, Y, Z, \rightarrow c, a, b$ [45,46]. Another assignment of optical axes is also generally used for KNB, namely $Y, X, Z \rightarrow (-a), b, c$ [39,41]. Unfortunately, we could not find a generally agreed assignment for this crystal in the literature (the two assignments can be even used by the same authors at different times: compare phase-matching curves in [45] and [39]) Nevertheless, all phase-matching calculations should be consistent as long as the assignment of axes is used consistently [47]. Thus, we decided to use the assignment that is implemented in the SNLO software [48], namely, $X, Y, Z, \rightarrow c, a, b$. For c-LNB, a uniaxial crystal, the selection of the phase-matching plane is straightforward. The most efficient type-I phase matching occurs in the ($-Y$, Z) plane ($\varphi = -90°$,θ can be varied) [40].

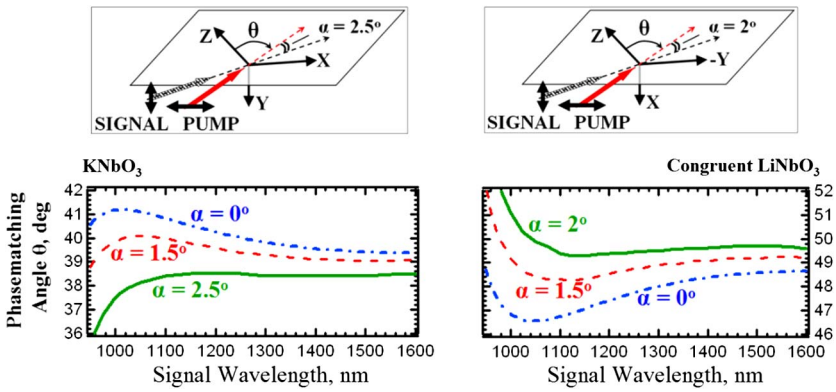

Fig. 1. Phase-matching curves for type I OPA in KNB (left) and c-LNB (right) pumped at 800 nm, at corresponding internal signal–pump noncollinear angles α. Top row, schemes corresponding to noncollinear geometry of pump and signal showing the noncollinear angle α and beam orientations with respect to the crystal axes; double arrows show the directions of polarization for signal and pump [48]. Reprinted from [49].

Phase-matching curves (Fig. 1) for the two crystals, calculated for type-I OPA (800 nm pump, o-signal + o-idler = e-pump), with the help of the SNLO software package [48] show that a certain signal-pump noncollinear angle exists at which phase-matching curves possess almost zero slope over a broad wavelength range (i.e., the phase-matching angle θ varying only within ~0.3°). Thus simultaneous amplification of near-IR white-light (WL) continuum in the ~1100–1600 nm wavelength region is expected from a NOPA based on these crystals.

3. EXPERIMENTAL REALIZATION OF NEAR-IR NONCOLLINEAR OPTICAL PARAMETRIC AMPLIFIER BASED ON BULK $LiNbO_3$ AND $KNbO_3$

The experimental setup for the realization of an ultrabroadband near-IR NOPA based on a KNB or a c-LNB crystal is very similar to that for KTP-NOPA (Fig. 2), with the difference of the external, and correspondingly, internal signal–pump noncollinear angles. The source of 800 nm pulses (~150 fs, 1 kHz, >600 μJ) is the oscillator–regenerative-amplifier system (Alpha-1000, BMI-Coherent), described previously [50]. The KNB crystal (2.46 mm thick) is cut for phase matching in the ZX (BC) plane at $\theta = 38°$, and the c-LNB crystal (2 mm thick) is cut for phase matching in the (YZ)—plane at $\theta = 48°$. A small portion of the 800 nm pulse energy (<5 μJ) was used to generate WL continuum pulses from a 2 mm thick sapphire plate. Before the nonlinear crystal, the pump pulses

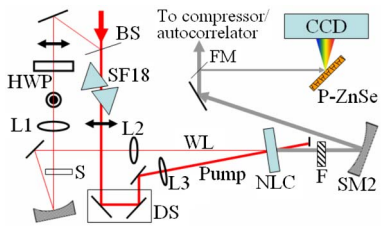

Fig. 2. Experimental setup for the proof-of-principle demonstration of near-IR NOPA based on KNB or c-LNB: BS, beam splitter; DS, delay stage; F, long-pass filter; FM, flip-mirror; HWP, half-wave plate; L, lenses; NLC, nonlinear optical crystal (KNB or c-LNB); P-ZnSe, polycrystalline ZnSe crystal; S, 2 mm sapphire plate; SF18, equilateral prisms; SM, spherical mirrors; WL, white-light continuum. Double arrows and dotted circles represent polarization of the beams in and normal to the plane of the drawing, respectively.

were passed through two SF18-prisms (face size 25 mm) in order to stretch them from ~150 fs to ~400–500 fs for better temporal overlap with the WL seed pulses [34]. The energy of the pump pulses at the nonlinear crystals was ~35 μJ, and the peak intensity was ~150 GW/cm^2, below the reported damage thresholds [41]. The external noncollinear angle between the signal seed and pump pulses was ~5° for KNB-NOPA and ~4° for c-LNB-NOPA, corresponding to internal noncollinear angles of ~2.4–2.5° for KNB and ~1.9–2.0° for c-LNB, respectively. The internal phase-matching angle for the pump pulses was θ~38.5° for KNB and ~49.0° for c-LNB (Fig. 1). The amplified signal pulses were collimated with a spherical mirror and sent to either a spectrometer or a compressor–autocorrelator system. Spectral characterization of the signal pulses was carried out by measuring the second-harmonic spectra in reflection off the surface of a 2 mm thick polycrystalline ZnSe crystal [34,51] with a CCD spectrograph, by doubling the wavelength axis and extracting the square root of second-harmonic intensity. Compression of the near-IR signal pulses was carried out in a fused-silica Brewster-cut prism pair, similar to the compression of pulses from KTP-NOPA [34].

Spectra of the near-IR signal pulses from both KNB-NOPA and c-LNB-NOPA are shown in Fig. 3(a). Both NOPAs provide ultrabroadband near-IR pulses covering the ~1000–1600 nm wavelength region [Fig. 3(a)] with a bandwidth >2900 cm^{-1}, or ~87 THz, corresponding to a transform limit (TL) ~8–10 fs, even broader than from periodically poled crystals [52]. The energy of amplified signal pulses from the KNB-NOPA is typically ~3–3.5 μJ, and ~1–1.5 μJ from the c-LNB-NOPA (corresponding to photon conversion efficiencies of ~13.5% and ~5.3%, respectively). The conversion efficiencies, as well as the relative spectral intensities, are in agreement with the calculated values of effective nonlinear coefficients (≈ – 4.2 pm/V for c-LNB and ≈6 pm/V for KNB) [48].

Compression of the ultrabroadband near-IR pulses provided ~38 fs pulsewidth [Fig. 3(b)]. Such long pulse durations of ~3.8 times TL are attributed to uncompensated pulse-front tilting of signal pulses in the noncollinear geometry, similar to the output of the ultrabroadband KTP-NOPA [34,35].

In order to correct for pulse-front tilting and achieve shorter pulse durations, we applied the method of pulse-front matching to correct the angular dispersion of the near-IR signal pulses from the double-stage LNB-KNB-NOPA (Fig. 4).

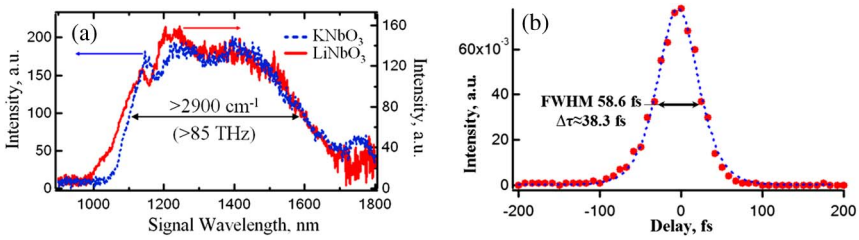

Fig. 3. Characterization of the ultrabroadband near-IR pulses from the single-stage NOPA (Fig. 2) based on c-LNB or KNB crystals. (a) Spectra of near-IR pulses from KNB-NOPA (dashed blue line) and c-LNB-NOPA (solid red line) derived from second-harmonic spectra measured at same integration times of the CCD camera from the polycrystalline ZnSe. (b) Autocorrelation of amplified signal pulses from c-LNB-NOPA measured on a 300 μm BBO crystal (red dots) together with a sech^2 fit yielding ~38.3 fs pulsewidth. Reprinted from [49].

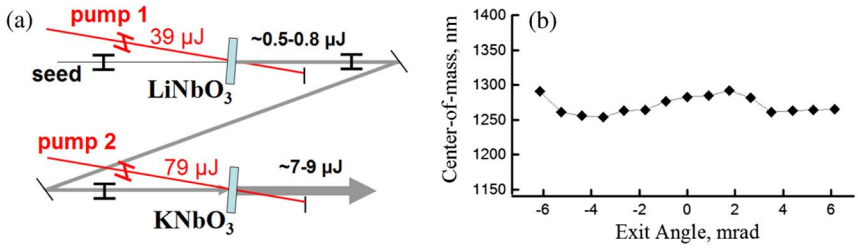

Fig. 4. (a) Schematic of the two-crystal NOPA based on successive amplification in LNB and KNB, with pulse-front matching implemented at both crystals. Pulse fronts of the signal and pump beams are shown. (b) Spectral center-of-mass values of signal pulses versus the exit angle measured by translating a ~100 μm slit 57 mm away from the KNB crystal.

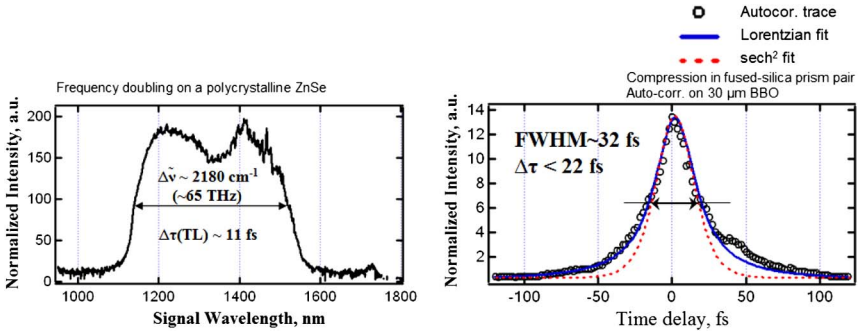

Fig. 5. Spectrum of near-IR pulses (left) generated from the two-stage LNB-KNB-NOPA with pulse-front matching and autocorrelation of these pulses (right) on a 30 μm thick BBO crystal (open circles), together with sech^2 (red dotted line) and Lorentzian (solid blue line) fits.

In the particular geometry described here, the pump pulses in the first stage (LNB crystal) were sent through an equilateral CaF_2 prism, and the pulse front was rotated in a +138 mm/ − 25 mm telescope. The pulse front of the pump pulses in the second stage was tilted by a combination of an equilateral fused silica prism and a +250 mm/ − 50 mm telescope [35]. The spectrum of the near-IR pulses from the two-crystal NOPA is narrower [$\Delta\nu \approx 66$ THz, or $\Delta\tilde{\nu} \approx 2200$ cm^{-1}, Fig. 5(a)] compared to the bandwidths generated from the single-stage NOPA's [Fig. 3(a)]. The relative narrowing can be explained by the partial chirping that the near-IR pulses undergo in the LNB crystal and other optics before arriving at the second NOPA-stage in KNB. The pulse-front matching considerably suppressed the angular dispersion of the amplified signal pulses after the second NOPA stage, as confirmed by measuring the dependence of the center of mass of the signal second-harmonic-generation spectra as a function of the signal beam exit angle [Fig. 4(b)] [35].

The compression of the amplified signal in the same arrangement (two Brewster-angle fused silica prisms) leads to pulse durations <22 fs, which is <2 × TL [compare to ~3.8 × TL for non-pulse-front-matched LNB-NOPA, Fig. 3(b)]. The interprism separation for the shortest pulses was ~44 cm, corresponding to second-order group-delay dispersion of −1760 fs^2 at 1300 nm [53]. The calculated third-order dispersion for the same interprism distance is +4490 fs^2, which makes a relatively high contribution at the generated bandwidths and is the most likely reason for not being able to approach the TL. We also note that the autocorrelation of the signal pulses after the KNB crystal can be fitted to a Lorentzian shape (yielding $\Delta\tau_{\text{Lorentz}}$~16 fs) much better than to a sech^2 function ($\Delta\tau_{\text{sech2}}$~21 fs, Fig. 5). Such a behavior can be explained by the exponential-like shape of the near-IR pulse spectrum at the edges.

In conclusion, we have demonstrated the broadband amplification of near- IR pulses centered at ~1300 nm with a bandwidth that supports transform-limited pulse durations of ~11 fs, corresponding to ~2.7 optical cycles, in a two-crystal NOPA based on bulk LNB and KNB. By correcting for pulse-front tilt we achieve compression to pulse durations <22 fs (~5.1 cycles). The described scheme is relatively simple, as it uses nonlinear crystals in the bulk forms. The compressibility

of pulses when pulse-front matching is applied suggests that the near-IR NOPA described here can be scaled to higher pulse energies [54,55]. Potential limitations for energy scaling may be imposed by damage in the nonlinear materials. Further improvements may include using MgO-doped LNB crystal for higher damage thresholds. Recently we showed that broadband phase matching in LNB and KNB provides broadband mid-IR idler pulses [43]; future work may include direct seeding with broadband IR pulses [23].

ACKNOWLEDGMENTS

We acknowledge the financial support from NSF (grant CHE 0809838).

REFERENCES

1. T. Popmintchev, M. C. Chen, A. Bahabad, M. Gerrity, P. Sidorenko, O. Cohen, I. P. Christov, M. M. Murnane, and H. C. Kapteyn, "Phase matching of high harmonic generation in the soft and hard X-ray regions of the spectrum," Proc. Natl. Acad. Sci. USA **106**, 10516–10521 (2009).
2. C. Vozzi, F. Calegari, F. Frassetto, L. Poletto, G. Sansone, P. Villoresi, M. Nisoli, S. De Silvestri, and S. Stagira, "Coherent continuum generation above 100 eV driven by an IR parametric source in a two-color scheme," Phys. Rev. A **79**, 033842 (2009).
3. A. D. DiChiara, S. Ghimire, C. I. Blaga, E. Sistrunk, E. P. Power, A. M. March, T. A. Miller, D. A. Reis, P. Agostini, and L. F. DiMauro, "Scaling of high-order harmonic generation in the long wavelength limit of a strong laser field," IEEE J. Sel. Top. Quantum Electron. **18**, 419–433 (2012).
4. G. Cerullo and S. De Silvestri, "Ultrafast optical parametric amplifiers," Rev. Sci. Instrum. **74**, 1–18 (2003).
5. D. Brida, M. Marangoni, C. Manzoni, S. De Silvestri, and G. Cerullo, "Two-optical-cycle pulses in the mid-infrared from an optical parametric amplifier," Opt. Lett. **33**, 2901–2903 (2008).
6. O. Chalus, P. K. Bates, M. Smolarski, and J. Biegert, "Mid-IR short-pulse OPCPA with micro-joule energy at 100 kHz," Opt. Express **17**, 3587–3594 (2009).
7. C. Erny, C. Heese, M. Haag, L. Gallmann, and U. Keller, "High-repetition-rate optical parametric chirped-pulse amplifier producing 1 μJ, sub-100 fs pulses in the mid-infrared," Opt. Express **17**, 1340–1345 (2009).
8. O. Chalus, A. Thai, P. K. Bates, and J. Biegert, "Six-cycle mid-infrared source with 3.8 μJ at 100 kHz," Opt. Lett. **35**, 3204–3206 (2010).
9. F. Junginger, A. Sell, O. Schubert, B. Mayer, D. Brida, M. Marangoni, G. Cerullo, A. Leitenstorfer, and R. Huber, "Single-cycle multiterahertz transients with peak fields above 10 MV/cm," Opt. Lett. **35**, 2645–2647 (2010).
10. J. Darginavicius, G. Tamosauskas, A. Piskarskas, and A. Dubietis, "Generation of 30 fs ultraviolet pulses by four-wave optical parametric chirped pulse amplification," Opt. Express **18**, 16096–16101 (2010).
11. D. Brida, C. Manzoni, G. Cirmi, M. Marangoni, S. Bonora, P. Villoresi, S. De Silvestri, and G. Cerullo, "Few-optical-cycle pulses tunable from the visible to the mid-infrared by optical parametric amplifiers," J. Opt. **12**, 013001 (2010).
12. A. P. Piskarskas, A. P. Stabinis, and V. Pyragaite, "Ultrabroad bandwidth of optical parametric amplifiers," IEEE J. Quantum Electron. **46**, 1031–1038 (2010).
13. V. Petrov, M. Ghotbi, O. Kokabee, A. Esteban-Martin, F. Noack, A. Gaydardzhiev, I. Nikolov, P. Tzankov, I. Buchvarov, K. Miyata, A. Majchrowski, I. V. Kityk, F. Rotermund, E. Michalski, and M. Ebrahim-Zadeh, "Femtosecond nonlinear frequency conversion based on BiB_3O_6," Laser Photon. Rev. **4**, 53–98 (2010).
14. M. Levenius, V. Pasiskevicius, F. Laurell, and K. Gallo, "Ultrabroadband optical parametric generation in periodically poled stoichiometric $LiTaO_3$," Opt. Express **19**, 4121–4128 (2011).
15. E. Riedle, M. Beutter, S. Lochbrunner, J. Piel, S. Schenkl, S. Sporlein, and W. Zinth, "Generation of 10 to 50 fs pulses tunable through all of the visible and the NIR," Appl. Phys. B **71**, 457–465 (2000).
16. L. Hongjun, Z. Wei, C. Guofu, W. Yishan, C. Zhao, and R. Chi, "Investigation of spectral bandwidth of optical parametric amplification," Appl. Phys. B **79**, 569–576 (2004).
17. A. Shirakawa, I. Sakane, and T. Kobayashi, "Pulse-front-matched optical parametric amplification for sub-10 fs pulse generation tunable in the visible and near infrared," Opt. Lett. **23**, 1292–1294 (1998).
18. I. Nikolov, A. Gaydardzhiev, I. Buchvarov, P. Tzankov, F. Noack, and V. Petrov, "Ultrabroadband continuum amplification in the near infrared using BiB_3O_6 nonlinear crystals pumped at 800 nm," Opt. Lett. **32**, 3342–3344 (2007).
19. D. Brida, G. Cirmi, C. Manzoni, S. Bonora, P. Villoresi, S. De Silvestri, and G. Cerullo, "Sub-two-cycle light pulses at 1.6 μm from an optical parametric amplifier," Opt. Lett. **33**, 741–743 (2008).
20. M. Ghotbi, M. Beutler, V. Petrov, A. Gaydardzhiev, and F. Noack, "High-energy, sub-30 fs near-IR pulses from a broadband optical parametric amplifier based on collinear interaction in BiB_3O_6," Opt. Lett. **34**, 689–691 (2009).
21. N. Ishii, K. Kaneshima, K. Kitano, T. Kanai, S. Watanabe, and J. Itatani, "Sub-two-cycle, carrier-envelope phase-stable, intense optical pulses at 1.6 μm from a BiB_3O_6 optical parametric chirped-pulse amplifier," Opt. Lett. **37**, 4182–4184 (2012).
22. J. Darginavicius, G. Tamosauskas, A. Piskarskas, G. Valiulis, and A. Dubietis, "Generation of tunable few optical-cycle pulses by visible-to-infrared frequency conversion," Appl. Phys. B **108**, 1–7 (2012).
23. J. Darginavicius, N. Garejev, and A. Dubietis, "Generation of carrier-envelope phase-stable two optical-cycle pulses at 2 μm from a noncollinear beta-barium borate optical parametric amplifier," Opt. Lett. **37**, 4805–4807 (2012).
24. S. W. Huang, J. Moses, and F. X. Kärtner, "Broadband noncollinear optical parametric amplification without angularly dispersed idler," Opt. Lett. **37**, 2796–2798 (2012).
25. C. Manzoni, S. W. Huang, G. Cirmi, P. Farinello, J. Moses, F. X. Kärtner, and G. Cerullo, "Coherent synthesis of ultra-broadband optical parametric amplifiers," Opt. Lett. **37**, 1880–1882 (2012).
26. T. Fuji and T. Suzuki, "Generation of sub-two-cycle mid-infrared pulses by four-wave mixing through filamentation in air," Opt. Lett. **32**, 3330–3332 (2007).
27. D. Faccio, A. Grun, P. K. Bates, O. Chalus, and J. Biegert, "Optical amplification in the near-infrared in gas-filled hollow-core fibers," Opt. Lett. **34**, 2918–2920 (2009).
28. P. Zuo, T. Fuji, and T. Suzuki, "Spectral phase transfer to ultrashort UV pulses through four-wave mixing," Opt. Express **18**, 16183–16192 (2010).
29. E. Rubino, J. Darginavicius, D. Faccio, P. Di Trapani, A. Piskarskas, and A. Dubietis, "Generation of broadly tunable sub-30 fs infrared pulses by four-wave optical parametric amplification," Opt. Lett. **36**, 382–384 (2011).
30. T. Fuji and Y. Nomura, "Generation of phase-stable sub-cycle mid-infrared pulses from filamentation in nitrogen," Appl. Sci. **3**, 122–138 (2013).
31. D. Kraemer, R. Hua, M. L. Cowan, K. Franjic, and R. J. D. Miller, "Ultrafast noncollinear optical parametric chirped pulse amplification in $KTiOAsO_4$," Opt. Lett. **31**, 981–983 (2006).
32. G. Cirmi, D. Brida, C. Manzoni, M. Marangoni, S. De Silvestri, and G. Cerullo, "Few-optical-cycle pulses in the near-infrared from a noncollinear optical parametric amplifier," Opt. Lett. **32**, 2396–2398 (2007).
33. D. Brida, S. Bonora, C. Manzoni, M. Marangoni, P. Villoresi, S. De Silvestri, and G. Cerullo, "Generation of 8.5 fs pulses at 1.3 μm for ultrabroadband pump-probe spectroscopy," Opt. Express **17**, 12510–12515 (2009).
34. O. Isaienko and E. Borguet, "Generation of ultra-broadband pulses in the near-IR by non-collinear optical parametric amplification in potassium titanyl phosphate," Opt. Express **16**, 3949–3954 (2008).
35. O. Isaienko and E. Borguet, "Pulse-front matching of ultrabroadband near-infrared noncollinear optical parametric amplified pulses," J. Opt. Soc. Am. B **26**, 965–972 (2009).

36. H. K. Nienhuys and H. J. Bakker, "Noncollinear optical parametric amplification in potassium titanyl phosphate pumped at 800 nm," Appl. Opt. **47**, 2870–2873 (2008).
37. O. Isaienko and E. Borguet, "Ultra-broadband infrared pulses from a potassium-titanyl phosphate optical parametric amplifier for VIS-IR-SFG spectroscopy," in *Ultrafast Phenomena*, P. Corkum, S. De Silvestri, K. A. Nelson, E. Riedle, and R. W. Schoenlein, eds., Vol. **XVI** of Springer Series in Chemical Physics (Springer, 2009), pp. 777–779.
38. O. Isaienko, E. Borguet, and P. Vöhringer, "High-repetition-rate near-infrared noncollinear ultrabroadband optical parametric amplification in $KTiOPO_4$," Opt. Lett. **35**, 3832–3834 (2010).
39. V. Petrov, F. Rotermund, and F. Noack, "Generation of high-power femtosecond light pulses at 1 kHz in the mid-infrared spectral range between 3 and 12 μm by second-order nonlinear processes in optical crystals," J. Opt. A **3**, R1–R19 (2001).
40. V. G. Dmitriev, G. G. Gurzadyan, and D. N. Nikogosyan, *Handbook of Nonlinear Optical Crystals* (Springer, 1999).
41. S. Cussat-Blanc, A. Ivanov, D. Lupinski, and E. Freysz, "$KTiOPO_4$, $KTiOAsO_4$, and $KNbO_4$ crystals for mid-infrared femtosecond optical parametric amplifiers: analysis and comparison," Appl. Phys. B **70**, S247–S252 (2000).
42. F. Rotermund, V. Petrov, and F. Noack, "Femtosecond noncollinear parametric amplification in the mid-infrared," Opt. Commun. **169**, 183–188 (1999).
43. O. Isaienko and E. Borguet, "Ultra-broadband sum-frequency vibrational spectrometer of aqueous interfaces based on a non-collinear optical parametric amplifier," Opt. Express **20**, 547–561 (2012).
44. N. Umemura, K. Yoshida, and K. Kato, "Phase-matching properties of $KNbO_3$ in the mid-infrared," Appl. Opt. **38**, 991–994 (1999).
45. V. Petrov and F. Noack, "Mid-infrared femtosecond optical parametric amplification in potassium niobate," Opt. Lett. **21**, 1576–1578 (1996).
46. C. J. Fecko, J. J. Loparo, and A. Tokmakoff, "Generation of 45 femtosecond pulses at 3 μm with a $KNbO_3$ optical parametric amplifier," Opt. Commun. **241**, 521–528 (2004).
47. V. G. Dmitriev and D. N. Nikogosyan, "Effective nonlinearity coefficients for 3-wave interactions in biaxial crystals of $mm2$ point group symmetry," Opt. Commun. **95**, 173–182 (1993).
48. A. Smith, "SNLO software package," www.as-photonics.com.
49. O. Isaienko and E. Borguet, "Ultra-broadband near-IR noncollinear optical parametric amplification in potassium niobate and lithium niobate," in *in Conference on Lasers and Electro-Optics/International Quantum Electronics Conference*, OSA Technical Digest (CD) (Optical Society of America, 2009), paper CFC7.
50. D. Bodlaki and E. Borguet, "Picosecond infrared optical parametric amplifier for nonlinear interface spectroscopy," Rev. Sci. Instrum. **71**, 4050–4056 (2000).
51. T. D. Chinh, W. Seibt, and K. Siegbahn, "Dot patterns from second-harmonic and sum-frequency generation in polycrystalline ZnSe," J. Appl. Phys. **90**, 2612–2614 (2001).
52. O. Y. Jeon, M. J. Jin, H. H. Lim, B. J. Kim, and M. Cha, "Broadband optical parametric amplification at the communication band with periodically poled lithium niobate," Opt. Express **14**, 7210–7215 (2006).
53. R. L. Fork, O. E. Martinez, and J. P. Gordon, "Negative dispersion using pairs of prisms," Opt. Lett. **9**, 150–152 (1984).
54. P. Tzankov, J. Zheng, M. Mero, D. Polli, C. Manzoni, and G. Cerullo, "300 μJ noncollinear optical parametric amplifier in the visible at 1 kHz repetition rate," Opt. Lett. **31**, 3629–3631 (2006).
55. J. A. Fulop, Z. Major, A. Henig, S. Kruber, R. Weingartner, T. Clausnitzer, E. B. Kley, A. Tunnermann, V. Pervak, A. Apolonski, J. Osterhoff, R. Horlein, F. Krausz, and S. Karsch, "Short-pulse optical parametric chirped-pulse amplification for the generation of high-power few-cycle pulses," New J. Phys. **9**, 438 (2007).